1. Supplementary Figures and Legends

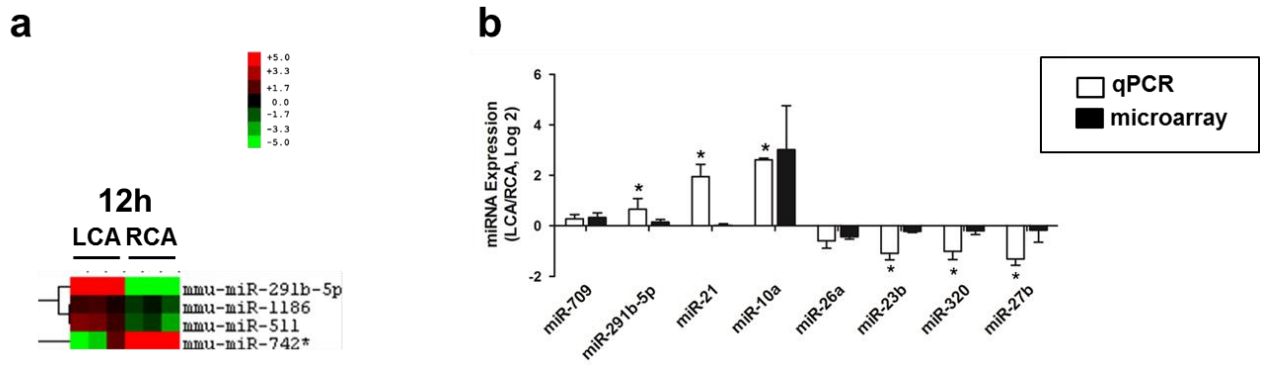

Supplementary Figure S1: Identification of mechanosensitive endothelial miRNAs *in vivo.* **(a)** Endothelial-enriched total RNAs obtained from intima of mouse (C57BL/6) left carotid (flow-disturbed LCA) and right carotid (contralateral control, RCA) at 12 post-ligation, were analyzed by gene array (Illumina BeadChip). Hierarchical clustering analyses of mechanosensitive miRNAs found in LCA endothelium compared to that of RCA are shown as heat maps. The color represents the expression level of the gene. Red represents high expression, while green represents low expression. The expression levels are continuously mapped on the color scale provided at the top of the figure. Each column represents a single sample pooled from 3 different LCAs or RCAs, and each row represents a single miRNA probe. **(b)** Also, 9 additional miRNAs, which did not show significant mechanosensitivity in the array study but were of potential relevance in endothelial biology, were tested (n=5; data shown as means ± s.e.m.; *, $p<0.05$ as determined by Student's *t*-test. Five of 9 miRNAs including miR-21 showed significant differences between LCA and RCA by qPCR, suggesting that our microarray results may underestimate the number of mechanosensitive miRNAs.

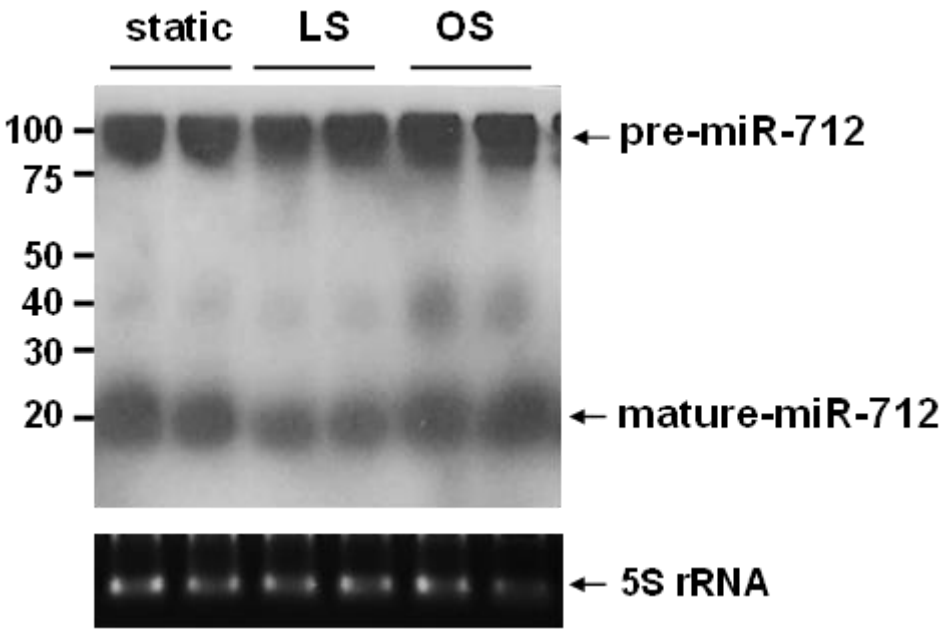

Supplementary Figure S2. **Oscillatory shear (OS) induces miR-712 in iMAECs.** Northern blot shows pre-miR-712 and mature-miR-712 in iMAEC exposed to static, laminar or oscillatory shear conditions for 24 h using DIG-labeled-LNA-miR-712 probe. Anti-DIG antibody conjugated to alkaline phosphatase was used for chemiluminescent detection. 5S rRNA was used as loading control for the experiment.

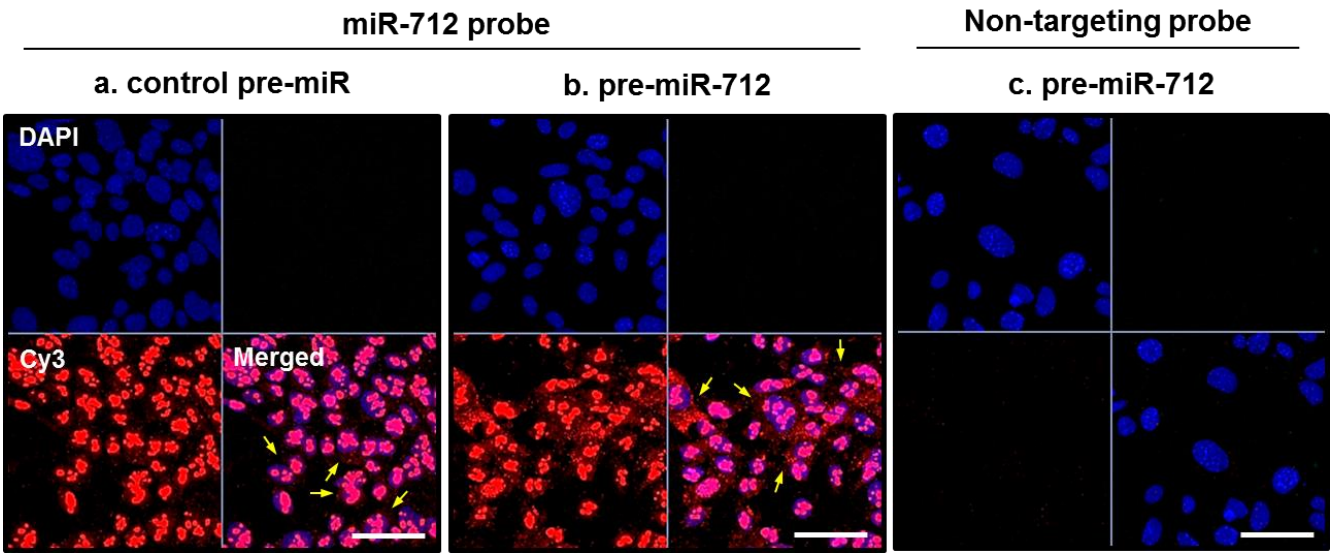

Supplementary Figure S3: *in situ* hybridization of miR-712 in iMAECs. iMAECs transfected with control (a) or pre-miR-712 (b, c) were used for *in situ* hybridization using digoxigenin (DIG)-labeled miR-712 probe (a, b) or DIG-labeled non-targeting probe (c) as a control. DIG was detected by anti-DIG antibody, which was visualized by Cy3 tyramide signal amplification method and imaged using confocal microscopy. Arrows indicate cytosolic miR-712; blue: DAPI stain. Scale bar=50μm.

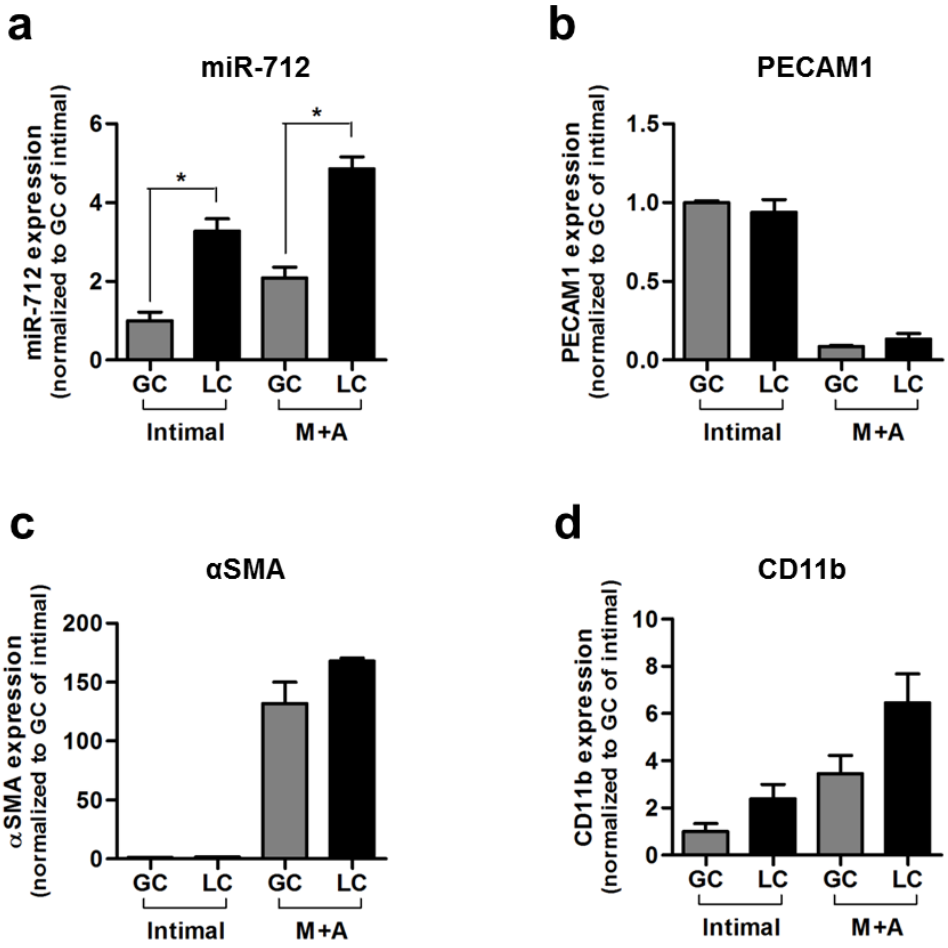

Supplementary Figure S4: Validation of miR-712 expression in natural *d-flow* regions of mouse aortic arch. Endothelial-enriched RNAs obtained from the natural *d-flow* (LC) and *s-flow* (GC) regions of mouse aortic arch were tested by qPCR to determine the expression of miR-712 (n=4, data shown as means ± s.e.m; *, $p<0.05$ as determined by Student's *t*-test). As a control, total RNAs obtained from the left-over samples following endothelial-enriched RNA preparation (media + adventitial regions: M+A) were used **(a)**. A panel of marker genes for endothelium (PECAM1), smooth muscle (αSMA) and immune cell (CD11b) was used to determine the purity of endothelial RNAs from the preparation **(b-d)**.

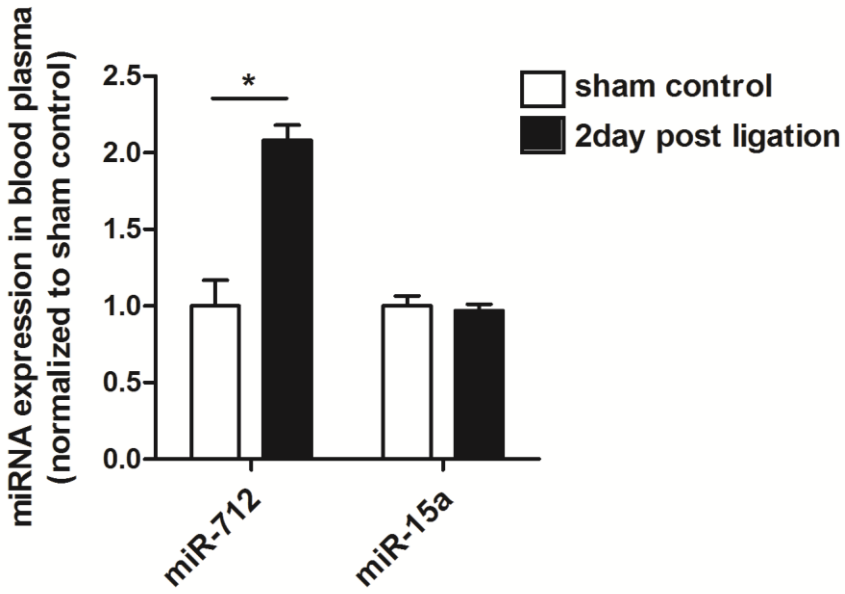

Supplementary Figure S5: Expression of miR-712 is increased in circulating blood plasma after 2-day partial ligation. C57bl6 mice underwent a partial carotid ligation or sham surgery and blood plasma was collected at two days post-ligation. Total RNA was extracted and expression of miR-712 and miR-15a (as a control) was determined by qPCR (n=3; data shown as means ± s.e.m; *, $p<0.05$ as determined by Student's *t*-test)

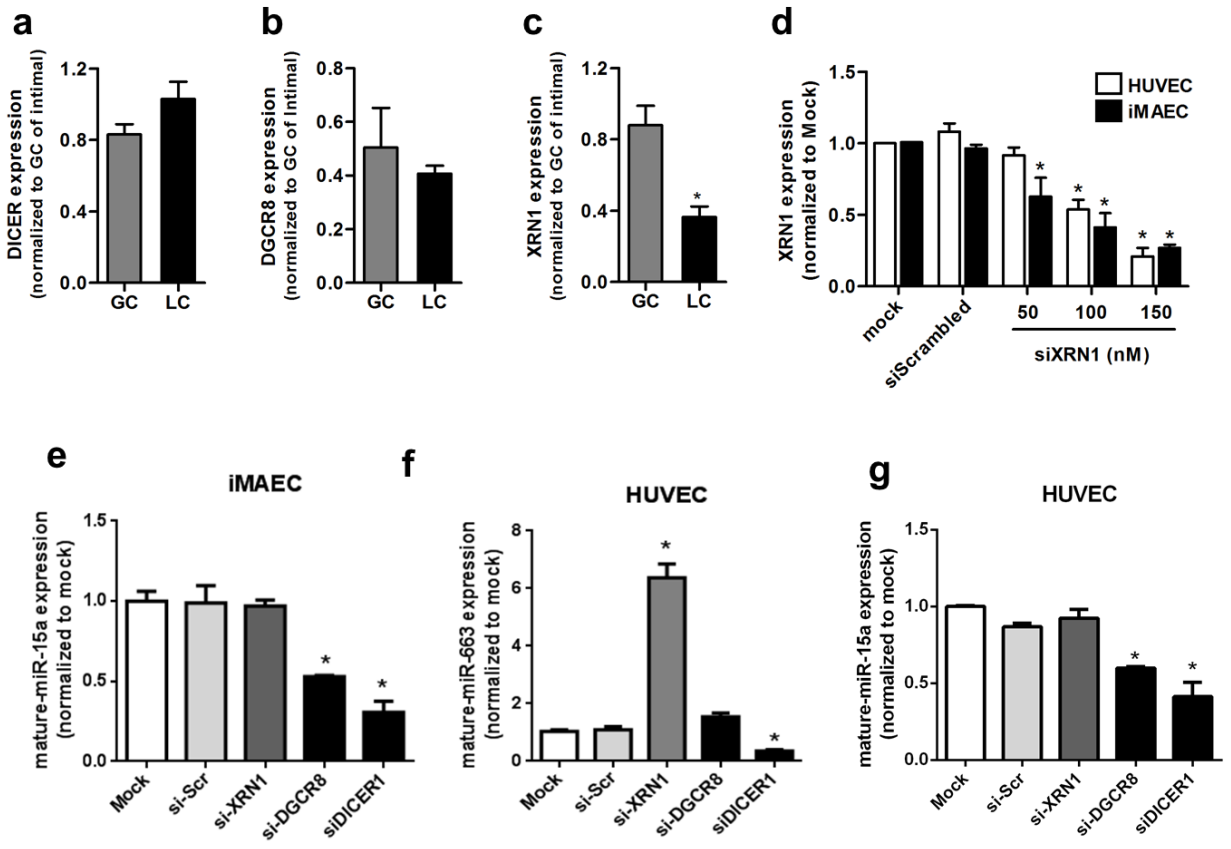

Supplementary Figure S6: Expression of microRNA processors (DICER1 and DGCR8) in the natural *d-flow* and *s-flow* regions of mouse aorta. Endothelial-enriched RNA from GC and LC regions of mouse aorta were used to determine the expression of *DICER1* and *DGCR8* by qPCR **(a-b)**. Expression of exonuclease *XRN1* was also determined by qPCR in LC and RC using the same samples **(c)**. Dose-dependent knockdown of XRN1 by siXRN1 in comparison to scrambled siRNA was determined in iMAECs and HUVECs **(d).** Expression of canonical miRNA (miR-15a) known to be regulated by the DGCR8/DROSHA and DICER-dependent pathway was determined by qPCR in iMAECs and HUVECs treated with siXRN1, siDGCR8, siDICER1 or scrambled control **(e and g)**. Expression of human miRNA (miR-663) was determined by qPCR in HUVECs treated with siXRN1, siDGCR8, siDICER1 or scrambled control **(f)** (n=3; data shown as means ± s.e.m; *, $p<0.05$ as determined by 1-way ANNOVA).

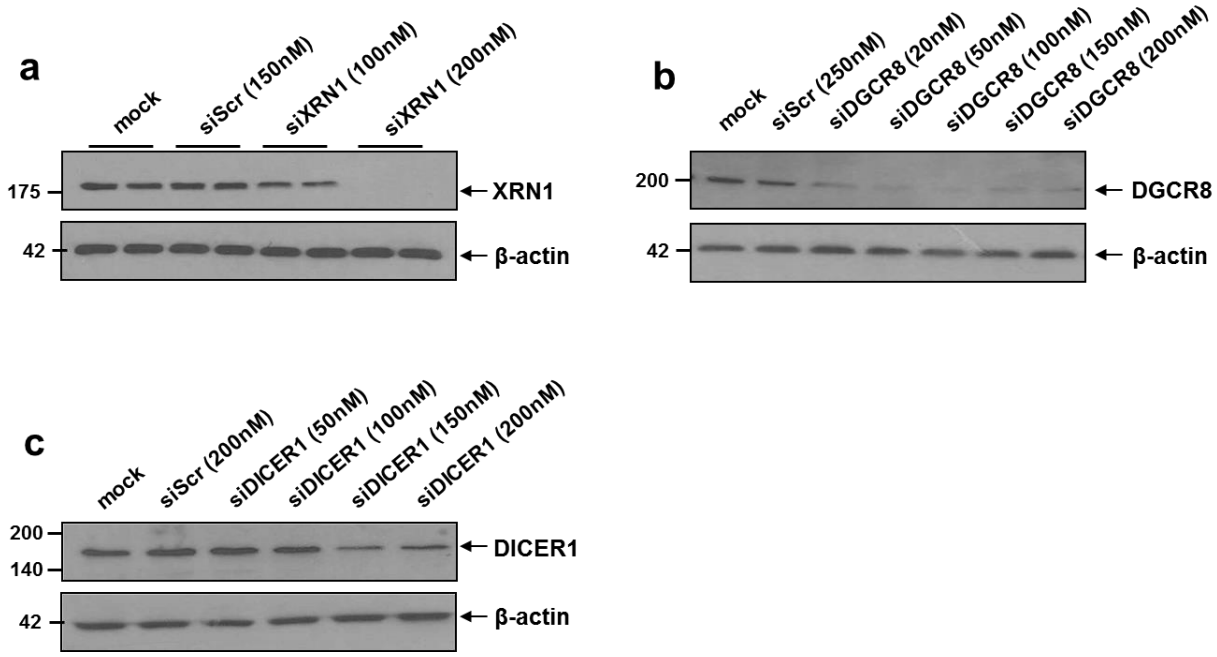

Supplementary Figure S7. Knockdown efficiency of siXRN1, siDGCR8, and siDICER1 in iMAECs. Representative Western blots show a dose-dependent decrease in the expression of **(a)** XRN1, **(b)** DGCR8 and **(c)** DICER1, respectively upon treatment with their specific siRNAs. Scrambled siRNA was used as negative control for these experiments. Full sized scans of all western blots are provided in Supplementary Figure S24.

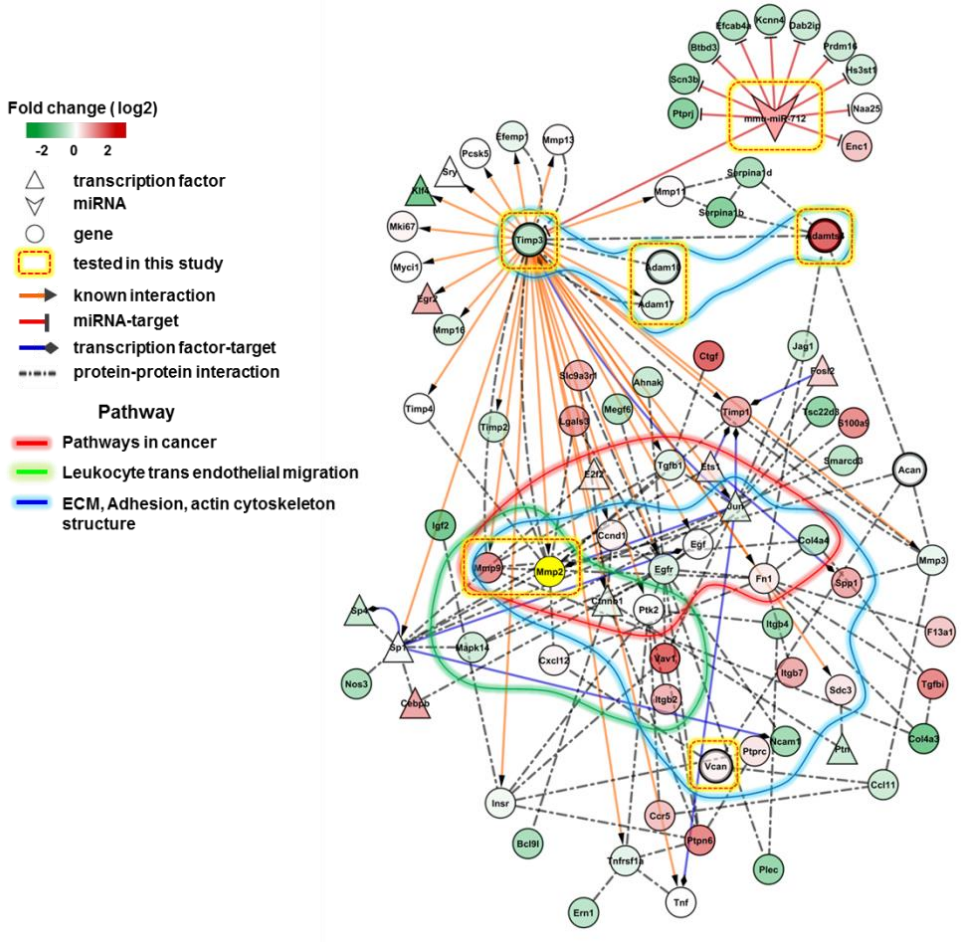

Supplementary Figure S8: miR-712 interactome. miR-712 predicted target gene list generated by TargetScan[60] was compared to the mechanosensitive gene list that we previously generated *in vivo* using the same mouse model[1], narrowing it to 11 potential miR-712 targets (shown by red arrows). In parallel, the previously generated mechanosensitive gene list was also analyzed by enriched KEGG pathway[61] using DAVID[62], providing an initial gene network map, which when compared against the filtered list of miR-712 target genes, revealed *TIMP3* as its potential target. The initial gene network map was then enriched by adding non-mechanosensitive genes with known associations to *TIMP3* using iHOP[63]. Additional interactions among TIMP3 associated genes were identified through physical protein-protein interaction (PPI) (ftp://ftp.ncbi.nih.gov/gene/GeneRIF/), transcription factor-target relations (TF-target)[64]. For clarity, the genes that were not directly connected to the TIMP3 network were excluded; resulting in the final network of miR-712/TIMP3 interactome consisted of 84 genes.

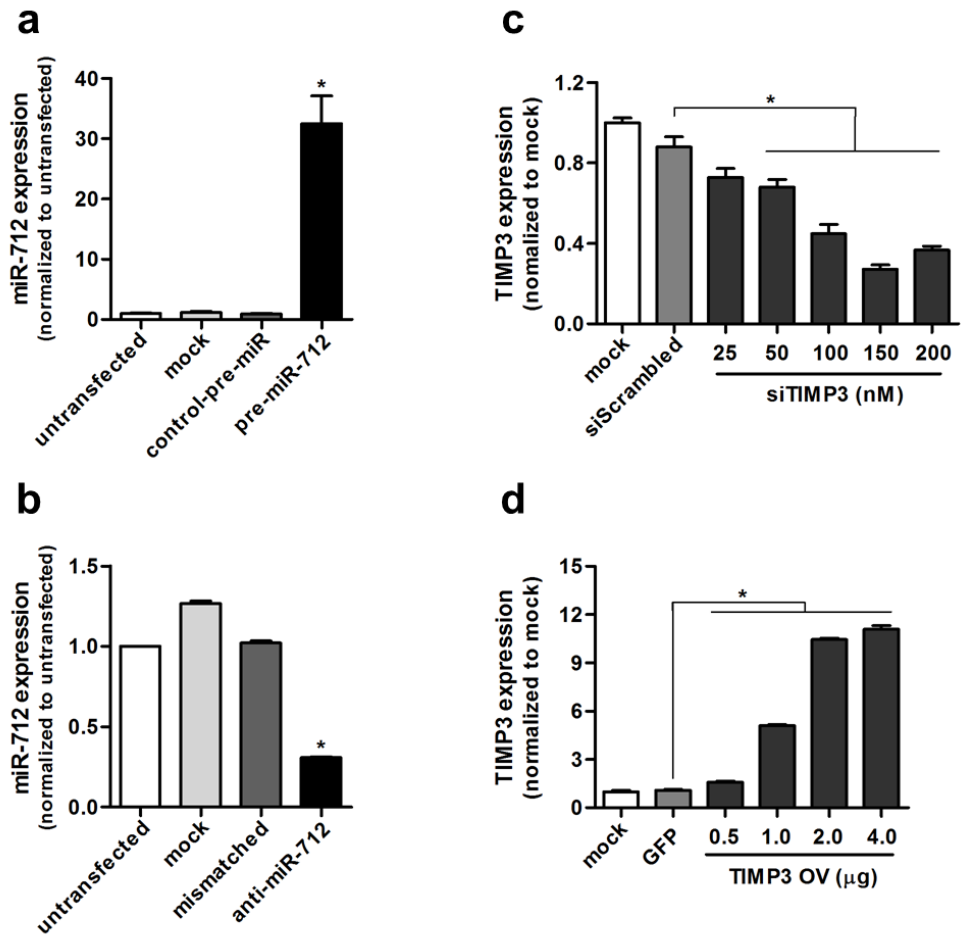

Supplementary Figure S9: Modulation of expression of miR-712 and TIMP3 by pre-miR-712, anti-miR-712, TIMP3 siRNA and TIMP3 overexpression plasmid in iMAECs. Pre-miR-712 or control-pre-miR (20nM) was transfected in iMAECs using Oligofectamine and expression of mature miR-712 was assessed by qPCR (*n=4*; data shown as means ± s.e.m; ***, p<0.05* as determined by Student's *t*-test) **(a)**. Anti-miR-712 or mismatched control (400nM) was transfected in iMAECs using Oligofectamine and expression of miR-712 was assessed by qPCR (n=4; data shown as means ± s.e.m; **, p<0.05 as determined by Student's *t*-test) **(b)**. A dose curve of siRNA for TIMP3 (from 25nM to 200 nM) was used to optimize the dose of siRNA in iMAECs. siRNA for TIMP3 or scrambled control was transfected in iMAECs using Oligofectamine and expression of TIMP3 was assessed by qPCR after 24 h of transfection **(c)**. iMAECs were transfected with mouse TIMP3 (0.5μg to 4 μg) or a control GFP expression vector using Amaxa nucleofection kit and expression of TIMP3 was determined by qPCR after 36 h (*n=4*) **(d)**.

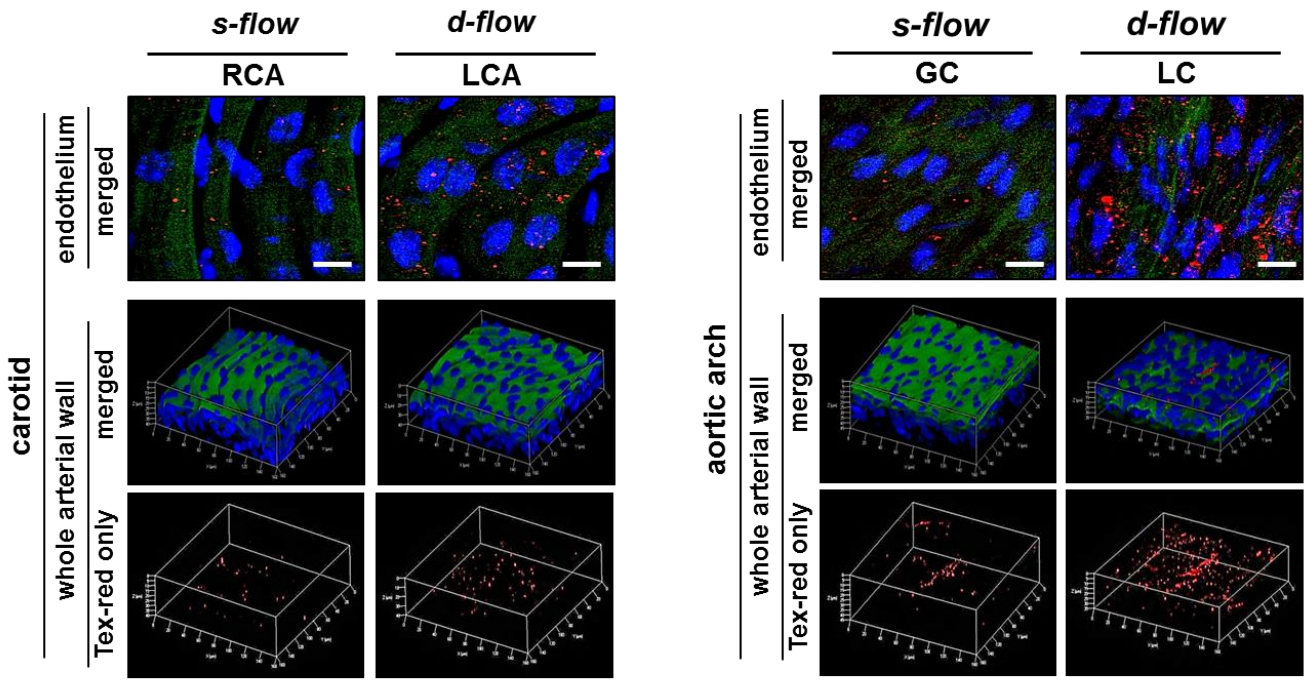
s-flow
d-flow
RCA
LCA
GC
LC
carotid
aortic arch
endothelium
whole arterial wall
merged
Tex-red only
Tex-red-615-anti-miR
Elastic lamina
Nucleus

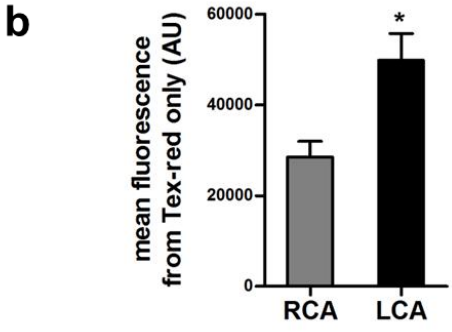
b
mean fluorescence from Tex-red only (AU)
60000
40000
20000
0
*
RCA
LCA

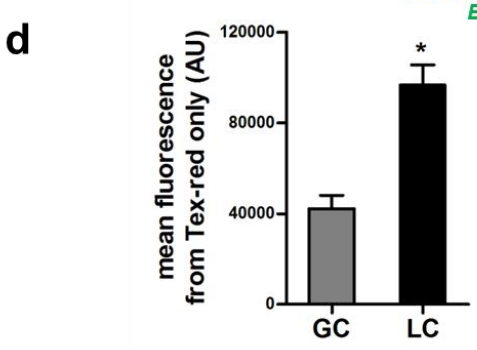
d
mean fluorescence from Tex-red only (AU)
120000
80000
40000
0
*
GC
LC

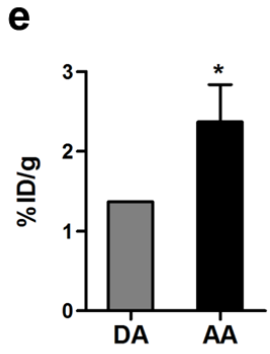
e
%ID/g
3
2
1
0
*
DA
AA

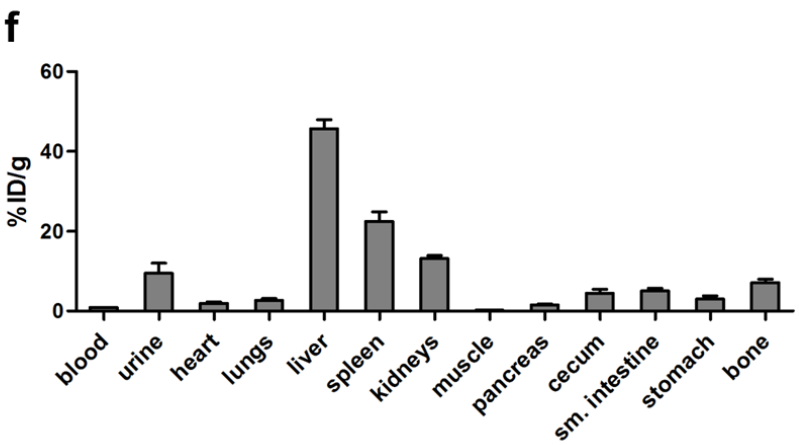
f
%ID/g
60
40
20
0
blood
urine
heart
lungs
liver
spleen
kidneys
muscle
pancreas
cecum
sm. intestine
stomach
bone

Supplementary Figure S10: Preferential delivery of LNA-based anti-miR-712 to *d-flow* regions of mouse arteries *in vivo*. (a-d) Two days after partial carotid ligation, C57Bl6 mice were injected with TexRed-615-labeled anti-miR control (Exiqon) or saline was injected (*s.c.*). Carotid arteries (a, b) and aortic arch (c, d) were then dissected out 24 h later, and accumulated fluorescence signal (Red) was examined and quantified by *en face* confocal microscopy. Nuclear DAPI (blue) and autofluorescent elastic laminar (green) are also shown. Top row shows TexRed-anti-miR delivery within endothelial cells. Mid and bottom rows show 3D rendering of merged images and anti-miR signal, respectively, in the carotid wall. The mean fluorescence intensities of TexRed 615 in the arterial walls were quantified in (b) and (d) (n=3; data shown as means ± s.e.m; *, $p<0.05$ as determined by Student's *t*-test). White scale bar=10μm. **(e) and (f)** Following partial carotid ligation and high-fat diet for 2 weeks, $ApoE^{-/-}$ mice were injected with ^{64}Cu-labelled anti-miR-712 via tail-vein. After 3 hours, aortic trees including carotids were dissected and autoradiographed, which were used to quantitate percentage of injected dose per gram (%ID/g) (n=6; data shown as means ± s.e.m; **, $p<0.05$ as determined by Student's *t*-test) **(e)**. To determine additional biodistribution of ^{64}Cu-labelled anti-miR-712, other tissue samples were also excised, cleaned, weighted and radioactivity quantified by a gamma counter. The biodistribution is reported as percent injected radioactivity per gram (%ID/g) of tissue.

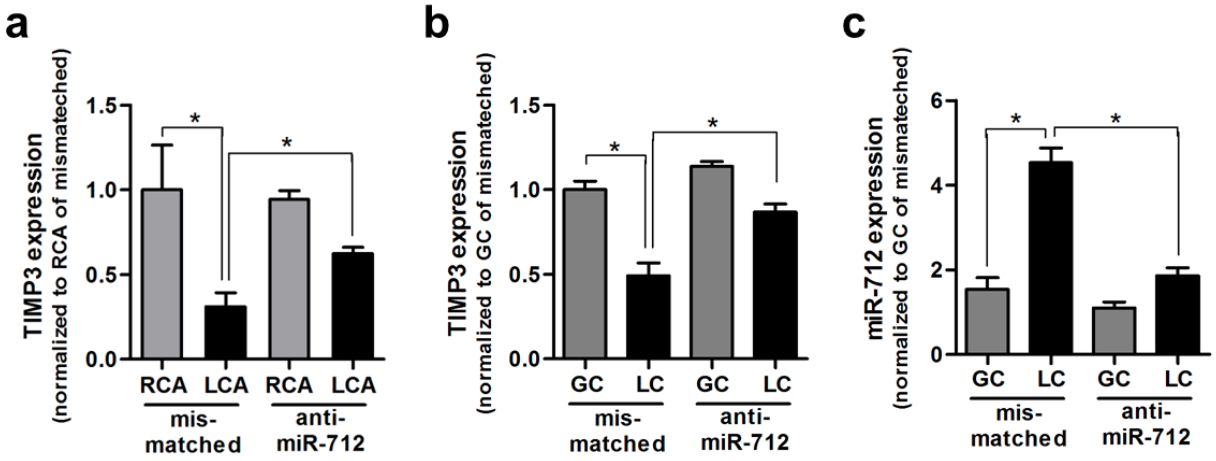

Supplementary Figure S11: Anti-miR-712 treatment inhibits endothelial expression of miR-712 and rescues TIMP3 expression in mouse arterial endothelium exposed to *d-flow in vivo*. C57Bl6 mice were injected with anti-miR-712 or mismatched control (5 mg/kg, *s.c.*) daily for 2 days, and followed by partial carotid ligation. Endothelial-enriched RNA from the LCA and RCA **(a)** as well from the natural *d-flow* (LC) and *s-flow* (GC) regions of the aortic arch were isolated and the expression of **(b)** TIMP3 and **(c)** miR-712 was determined by qPCR (n=4; data shown as means ± s.e.m; **, $p<0.05$ as determined by Student's *t*-test).

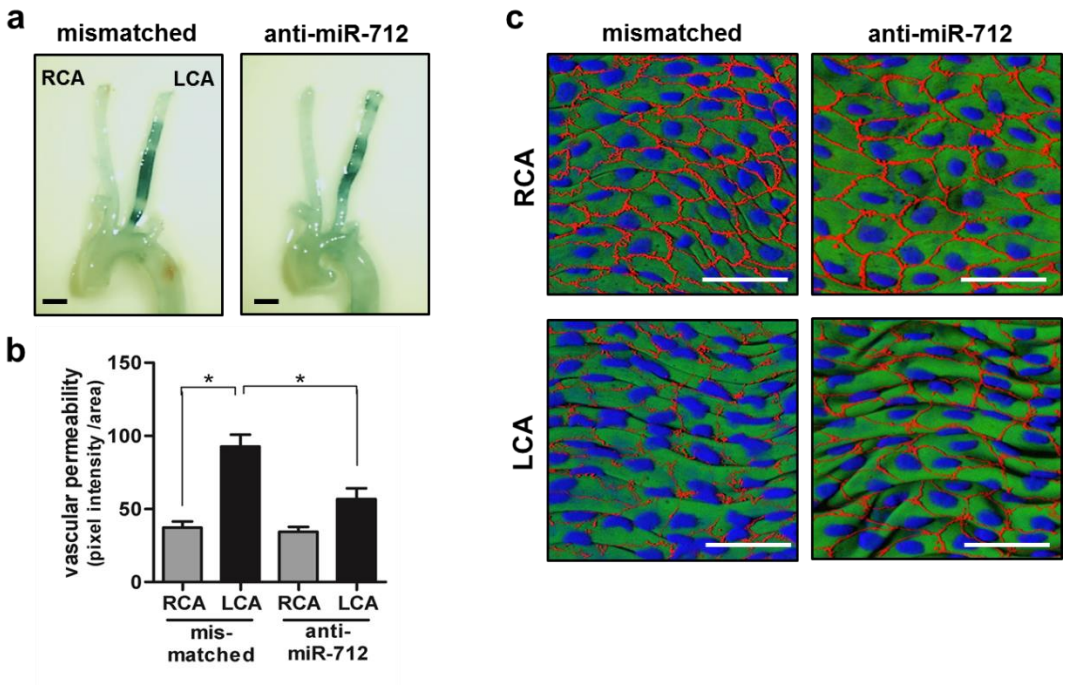

Supplementary Figure S12. Anti-miR-712 treatment inhibits (1) increased endothelial permeability and (2) reduced junctional VE-cadherin in partially ligated mouse LCA. (a-c) C57Bl6 mice were pre-treated with anti-miR-712 or mismatched control (5 mg/kg, *s.c.*), two times for 1 week. Partial carotid ligation was then performed and mice received two additional anti-miR and control injections. **(a, b)** One week after the ligation, 1% Evans Blue was injected via tail vein (100 μl/animal) and 30-min post-injection, animals were sacrificed and aortic trees were isolated, imaged by bright field microscopy **(a)** and Evans Blue uptake in the carotids was quantified by NIH Image J software. Scale bar=1mm. **(b)** (n=5; data shown as means ± s.e.m; *, $p<0.05$ as determined by Student's *t*-test). **(c)** Four days after the ligation**,** RCA and LCA were dissected out and stained with VE-cadherin antibody (Red) and imaged *en face* by confocal microscopy. Blue: DAPI nuclear staining; Green: autofluorescence of internal elastic lamina. Scale bar=50μm.

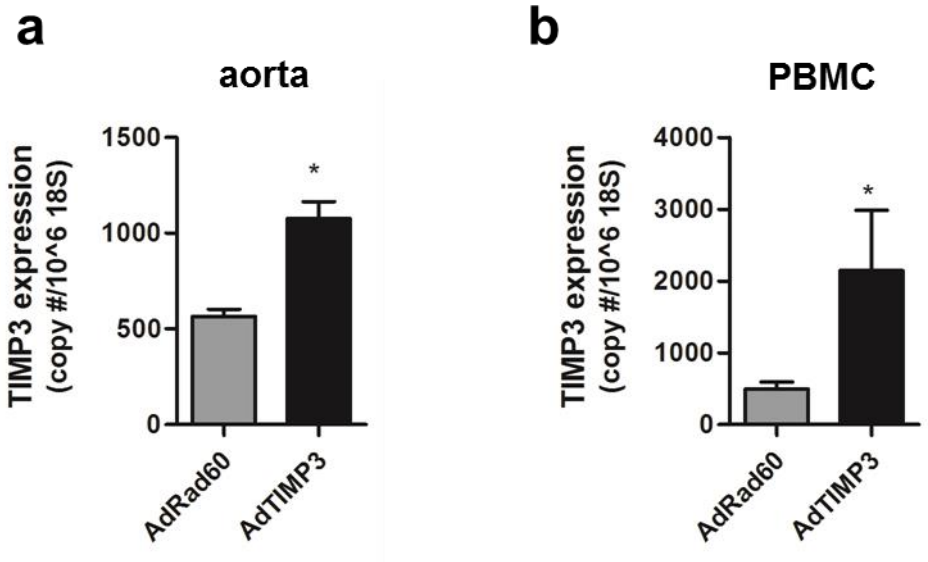

Supplementary Figure S13. AdTIMP3 treatment increased TIMP3 expression in the thoracic aorta and peripheral blood mononuclear cells (PBMCs) in C57Bl6 mice. Mice were injected with AdTIMP3 (10^8 pfu/animal) (AdTIMP3) or empty Ad vector control (AdRad60) via tail vein. After 5 days, total RNA was obtained from the **(a)** aorta and **(b)** PBMCs and expression TIMP3 was determined by qPCR (n=5; data shown as means ± s.e.m; *, $p<0.05$ as determined by Student's *t*-test).

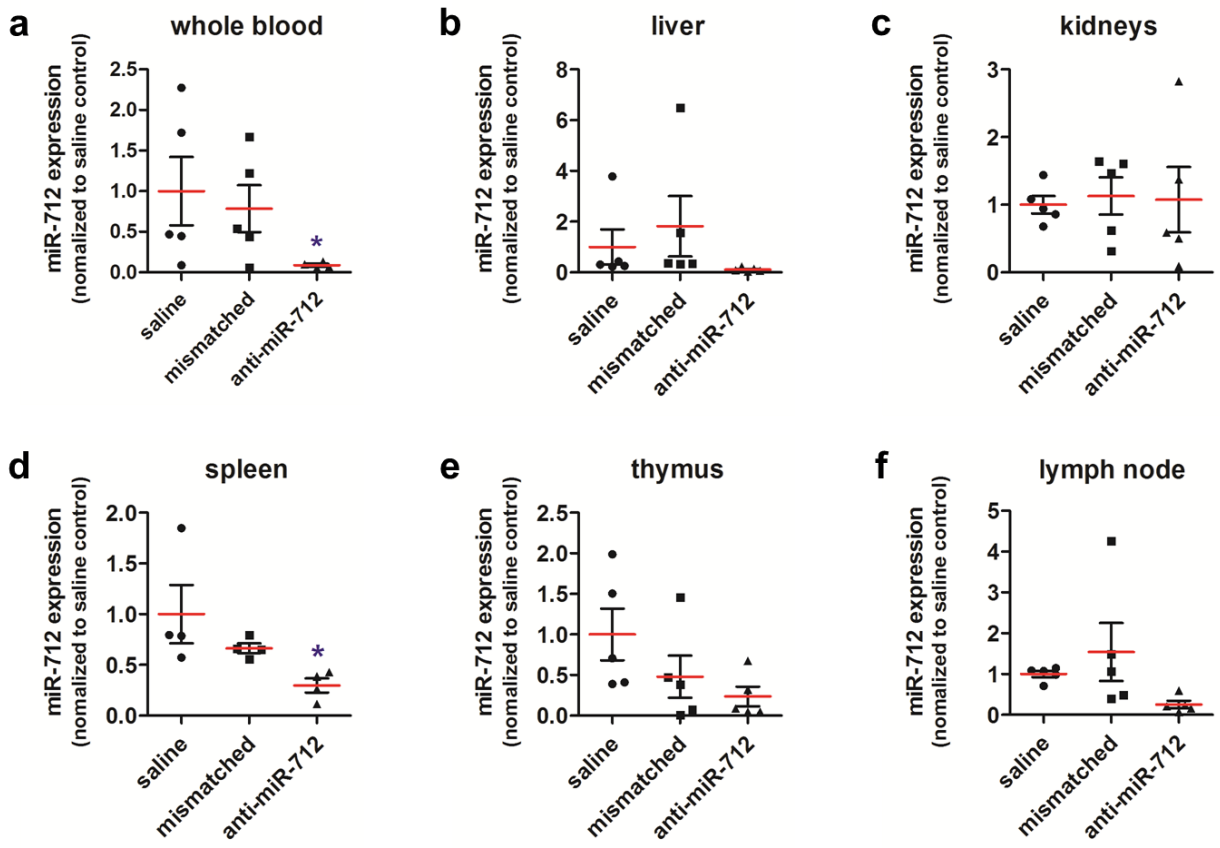

Supplementary Figure S14: Effect of anti-miR-712 treatment on expression of miR-712 in mouse tissues. *ApoE*$^{-/-}$ mice were pretreated twice with anti-miR-712 or mismatched control (5mg/kg each, *s.c.*) or saline on 1 and 2 days prior to partial ligation. Mice were then fed a high-fat diet and the anti-miR and control treatments were continued (twice a week *s.c.*) for one week. Animals were sacrificed and various tissues and whole blood were obtained, total RNA was extracted and expression of miR-712 was determined by qPCR. Graphs show relative expression of miR-712 in **(a)** whole blood; **(b)** liver; **(c)**, kidneys; **(d)** spleen; **(e)** thymus and **(f)** lymph node (n=4-5; data shown as means ± s.e.m; * *, $p<0.05$ as determined by Student's *t*-test).

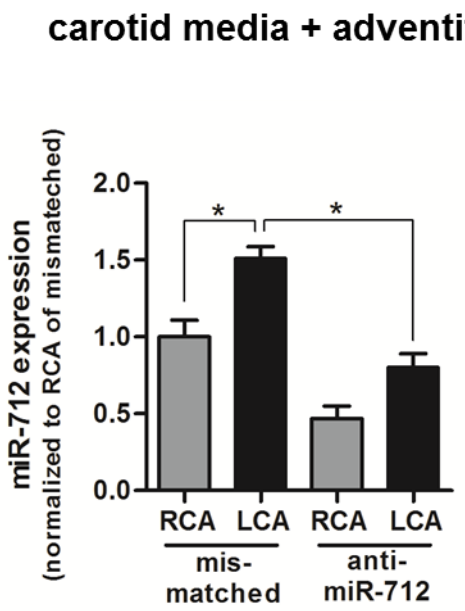

Supplementary Figure S15: Anti-miR-712 treatment inhibits expression of miR-712 in media and adventitia of carotid arterial walls *in vivo*. C57Bl6 mice were injected with anti-miR-712 or mismatched control (5 mg/kg, *s.c.*) daily for 2 days, and followed by partial carotid ligation. After collecting the endothelial-enriched RNA from the LCA and RCA, the left over samples (containing media and adventitia) were used for total RNA preparation and expression of miR-712 was determined by qPCR (n=5; data shown as means ± s.e.m; **, $p<0.05$ as determined by Student's *t*-test).

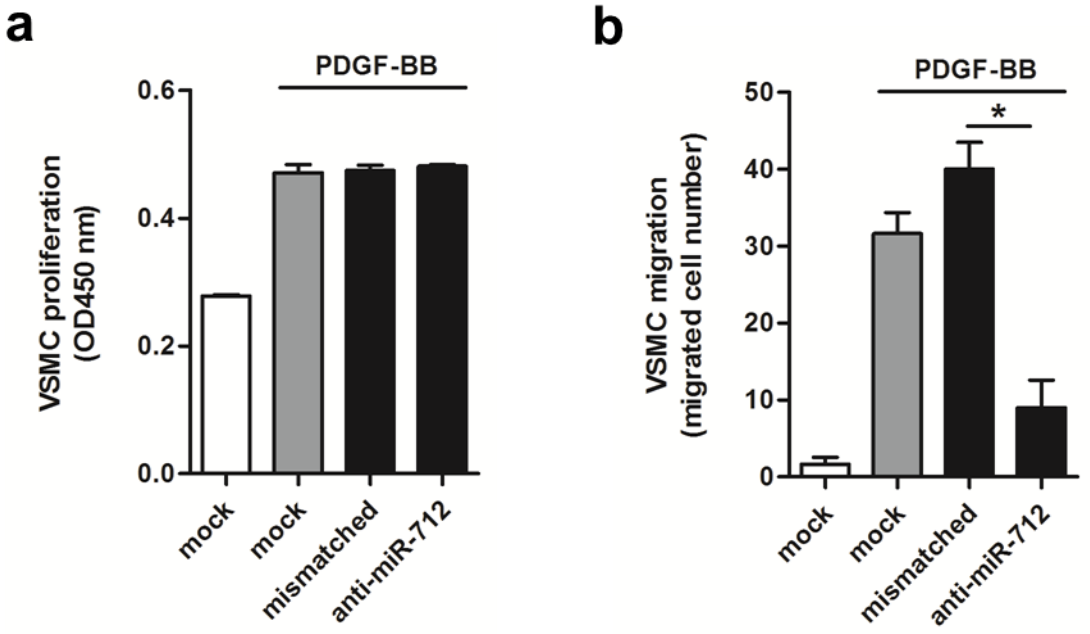

Supplementary Figure S16. miR-712 mediates mouse vascular smooth muscle cells (VSMC) migration, but not proliferation in response to PDGF. VSMCs transfected with anti-miR-712 or mismatched control for 24 h were treated with PDGF-BB (10ng/mL). Cell proliferation and migration were determined by water soluble Tetrazolium salts (WST1) assay (n=10) **(a)** and trans-well migration assay (n=5; data shown as means ± s.e.m; **, $p<0.05$ as determined by Student's *t*-test) **(b)**, respectively.

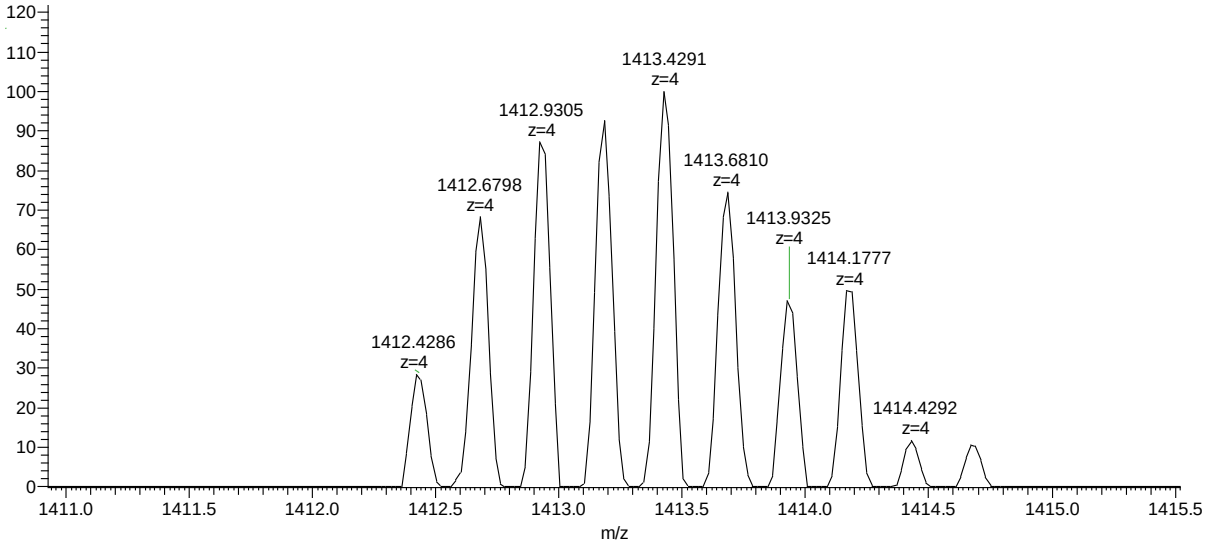

Supplementary Figure S17. Mass spectrum of anti-miR712-DOTA

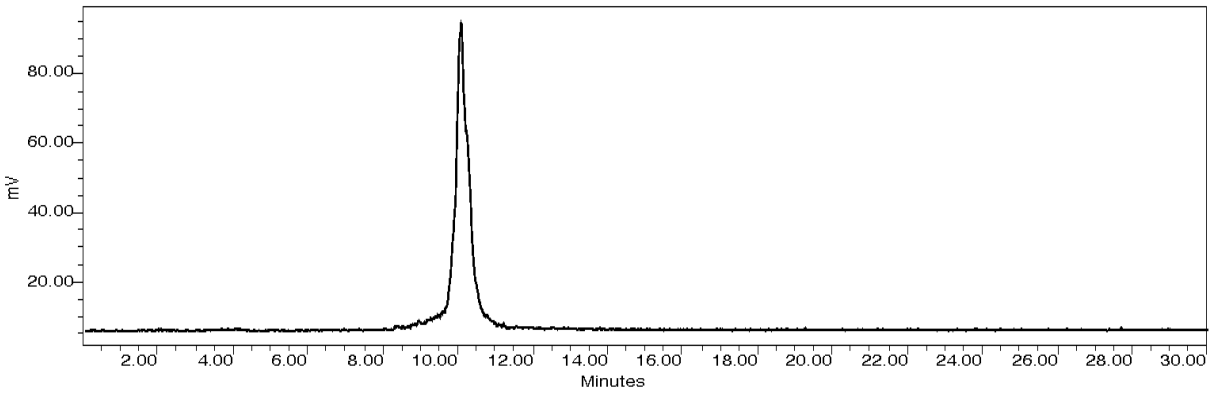

Supplementary Figure S18. Radiochromatogram of ^{64}Cu-labeled anti-miR712-DOTA. HPLC condition: column Clarity Oligo-PR (250x10.00 mm), gradient: 5 – 90% of solvent B for 0-30 min [(solvent A: 0.1 M triethylammonium acetate (TEAA), solvent B: acetonitrile)].

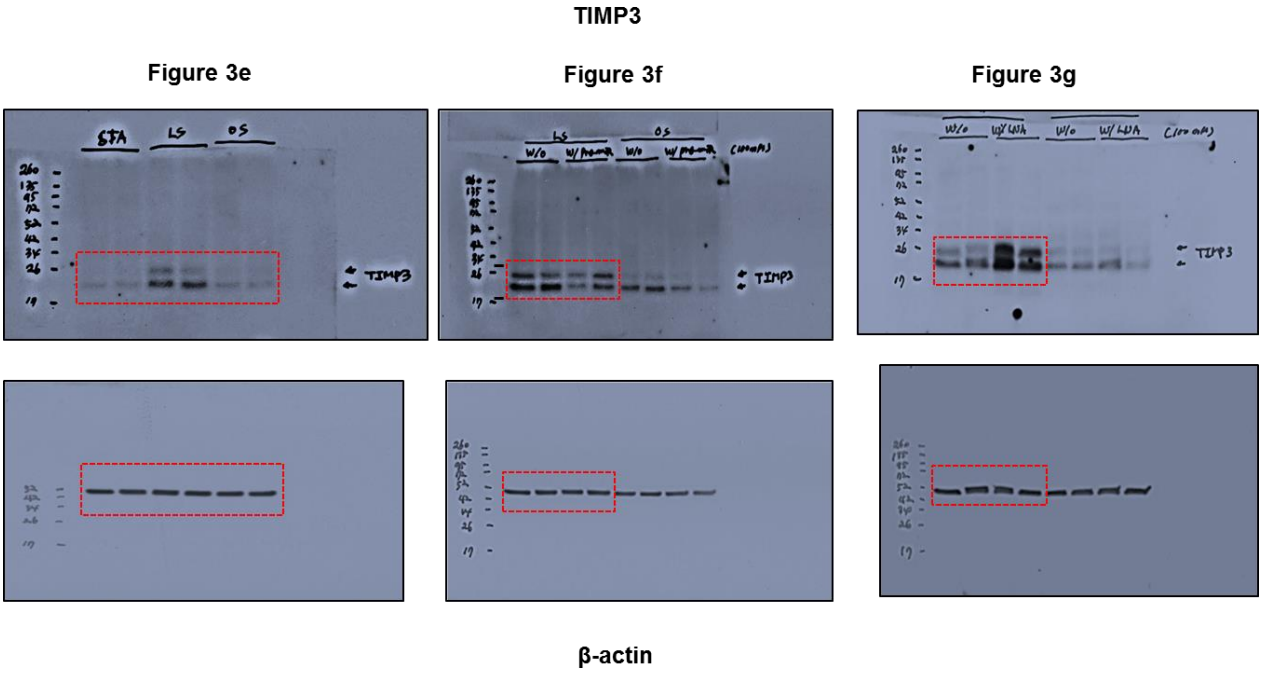

Supplementary Figure S19. **Full scans of the of Western Blots for TIMP3 and β-actin**

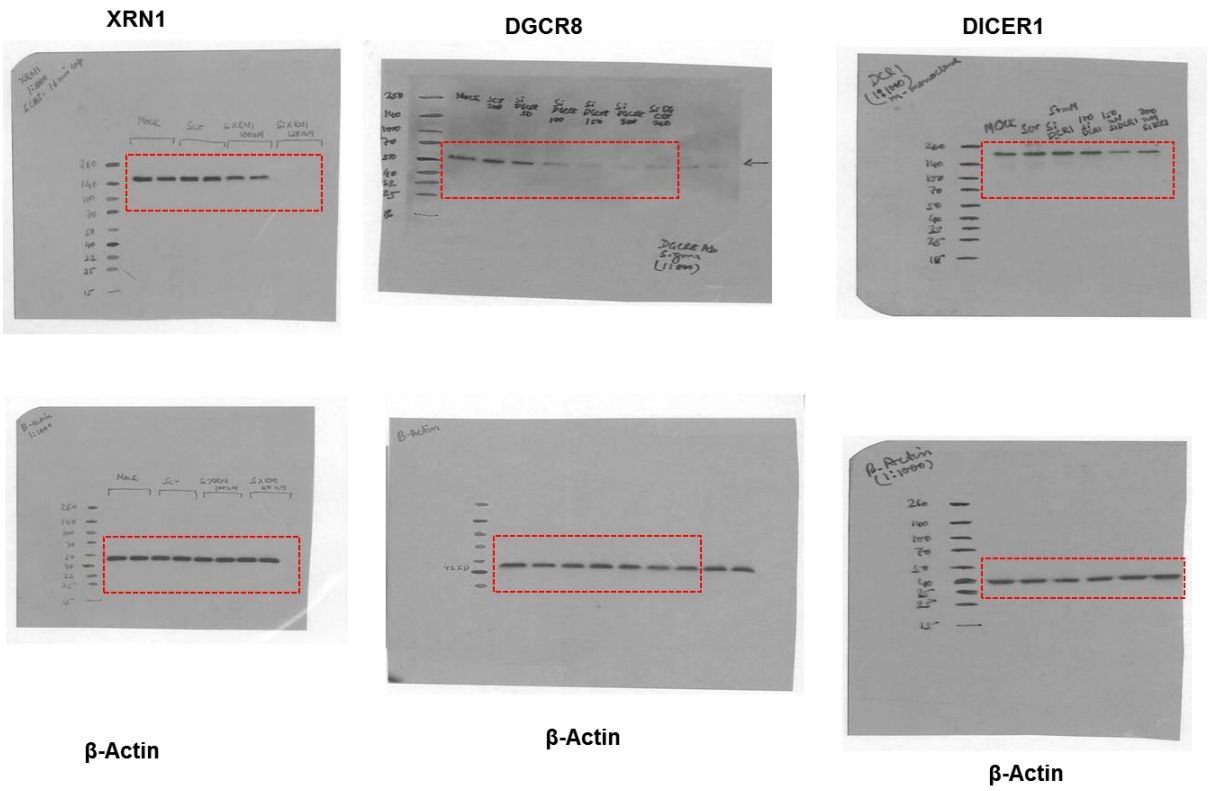

Supplementary Figure S 20. **Full scans of the Western Blots for XRN1, DGCR8, DICER1 and respective β-actin.**

2. Supplementary Tables

Supplementary Table S1. Fold-change expression of mechanosensitive miRNAs regulated by disturbed flow in mouse LCA compared to RCA endothelium.

Gene Name	LCA/RCA (Log2)	q-value (%)	Gene Name	LCA/RCA (Log2)	q-value (%)
Up-regulated by LCA 12h post-ligation			**Down-regulated by LCA 12h post-ligation**		
mmu-miR-291b-5p	4.10	0.00	mmu-miR-742*	-0.77	0.00
mmu-miR-511	1.19	0.00			
mmu-miR-1186	0.61	0.00			
Up-regulated by LCA 48h post-ligation			**Down-regulated by LCA 48h post-ligation**		
mmu-miR-712	3.98	0.00	mmu-miR-7a	-2.10	0.00
mmu-miR-330*	4.10	0.00	mmu-miR-29b	-1.87	0.00
mmu-miR-200c	3.88	0.00	mmu-miR-574-5p	-0.87	0.00
mmu-miR-92b	2.19	0.00	mmu-miR-327	-1.60	5.03
mmu-miR-223	1.92	0.00	mmu-let-7d	-1.01	5.03
solexa-1127-427	1.76	0.00	mmu-miR-195	-2.33	7.37
mmu-miR-615-5p	1.29	0.00	mmu-miR-26b	-1.67	7.37
mmu-miR-128a:9.1	0.99	0.00	mmu-miR-30c	-1.89	7.37
mmu-miR-93	0.93	0.00	mmu-miR-692	-0.79	7.37
solexa-284-1594	0.91	0.00	mmu-miR-509-5p	-0.71	7.37
mmu-miR-423-3p	0.88	0.00	mmu-miR-221	-1.66	8.43
mmu-miR-324-3p	0.78	0.00	mmu-miR-181d	-0.74	8.43
mmu-miR-146b	3.92	3.69	mmu-miR-691	-0.73	8.43
mmu-miR-699	3.67	3.69	mmu-miR-877*	-3.47	10.29
solexa-308-1456	0.95	3.69	mmu-miR-152	-2.03	10.29
mmu-miR-138*	0.90	3.69	mmu-miR-30d	-1.72	10.29
mmu-miR-210	0.64	3.69	mmu-miR-509-3p	-0.77	10.29
mmu-miR-669e	5.10	6.70	mmu-miR-20a*	-0.81	10.29
mmu-miR-770-5p	1.85	6.70			
solexa-200-2167	2.67	6.70			
mmu-miR-128	2.66	6.70			
mmu-miR-339-5p	1.11	6.70			
mmu-miR-703	0.61	6.70			
mmu-miR-342-3p	1.13	7.97			
mmu-miR-17*	3.35	9.83			
mmu-miR-296-5p	3.05	9.83			
mmu-miR-93*	0.96	9.83			

Supplementary Table S2. Serum lipid profile

Study	Group (n)	Total Cholesterol (mg/dL)	LDL (mg/dL)	HDL (mg/dL)	Triglycerides (mg/dL)
Acute	saline (10)	960.00±33.33	421.30±16.61	14.63±0.85	202.00±16.83
	mismatched (10)	954.90±26.11	401.10±12.49	13.72±1.32	196.20±25.15
	anti-miR-712 (10)	1051.00±47.74	412.80±28.37	17.16±0.72	218.00±20.79
Chronic	saline (5)	1332.00±44.74	1291.14±43.75	16.86±1.37	120.00±19.55
	mismatched (8)	1254.75±90.19	1209.50±89.69	18.25±0.93	135.00±13.46
	anti-miR-712 (10)	1343.70±134.40	1293.98±123.90	14.18±1.46	177.70±53.07

Serum lipid profile from two different studies: (1) **Acute:** ApoE$^{-/-}$ mice after partial carotid ligation were fed with a high-fat diet for 2 weeks (2) **Chronic:** ApoE$^{-/-}$ mice were fed western diet for 3 months. Animals were treated with either anti-miR-712, mismatched control or saline for the entire duration of the study. Blood collected immediately following sacrifice was used to measure total cholesterol, light-density lipoprotein (LDL), high-density lipoprotein (HDL) and triglycerides at Emory Cardiovascular Specialty Laboratories. (data shows means ± s.d.)

Supplementary Table S3. List and sequences of qPCR primers for validation of miRNA.

micro RNA	Forward Primer
mmu-miR-330*	5'-GCAAAGCACAGGGCCTGCAGAGA-3'
mmu-miR-712	5'-CTCCTTCACCCGGGCGGTACC-3'
mmu-miR-92b	5'-TATTGCACTCGTCCCGGCCTCC-3'
mmu-miR-223	5'-TGTCAGTTTGTCAAATACCCCA-3'
mmu-miR-770-5p	5'-AGCACCACGTGTCTGGGCCACG-3'
mmu-miR-138*	5'-CGGCTACTTCACAACACCAGGG-3'
mmu-miR-195	5'-TAGCAGCACAGAAATATTGGC-3'
mmu-miR-30c	5'-TGTAAACATCCTACACTCTCAGC-3'
mmu-miR-29b	5'-TAGCACCATTTGAAATCAGTGTT-3'
mmu-miR-26b	5'-TTCAAGTAATTCAGGATAGGT-3'
mmu-miR-221	5'-AGCTACATTGTCTGCTGGGTTTC-3'
mmu-let-7d	5'-AGAGGTAGTAGGTTGCATAGTT-3'
mmu-miR-574-5p	5'-TGAGTGTGTGTGTGTGAGTGTGT-3'
mmu-miR-511	5'-ATGCCTTTTGCTCTGCACTCA-3'
mmu-miR-709	5'-GGAGGCAGAGGCAGGAGGA-3'
mmu-miR-291b-5p	5'-GATCAAAGTGGAGGCCCTCTCC-3'
mmu-miR-21	5'-TAGCTTATCAGACTGATGTTGA-3'
mmu-miR-1186	5'-GAGTGCTGGAATTAAAGGCATG-3'
mmu-miR-26a	5'-TTCAAGTAATCCAGGATAGGCT-3'
mmu-miR-23b	5'-ATCACATTGCCAGGGATTACC-3'

mmu-miR-320	5'-AAAAGCTGGGTTGAGAGGGCGA-3'
mmu-miR-27b	5'-TTCACAGTGGCTAAGTTCTGC-3'
mmu-miR-128a-3p	5'-TCACAGTGAACCGGTCTCTTT-3'
mmu-miR-146b	5'-TGAGAACTGAATTCCATAGGCT-3'
mmu-miR-132	5'-TAACAGTCTACAGCCATGGTCG-3'
mmu-miR-342-3p	5'-TCTCACACAGAAATCGCACCCGT-3'
mmu-miR-423-3p	5'-AGCTCGGTCTGAGGCCCCTCAGT-3'
mmu-miR-7a	5'-TGGAAGACTAGTGATTTTGTTGT-3'
mmu-miR-327	5'-ACTTGAGGGGCATGAGGAT-3'
sno202	5'-GACTTGATGAAAGTACTTTTGAACCC-3'

Supplementary Table S4. List and sequences of qPCR primers for mRNA expression.

Primer Name	Sequences
TIMP3_F	5'-CACGGAAGCCTCTGAAAGTC-3'
TIMP3_R	5'-TCCCACCTCTCCACAAAGTT-3'
ADAM10_F	5'-GGGAAGAAATGCAAGCTGAA-3'
ADAM10_R	5'-CTGTACAGCAGGGTCCTTGAC-3'
ADAMTS4_F	5'-CTTCCTGGACAATGGTTATGG-3'
ADAMTS4_R	5'-GAAAAGTCGCTGGTAGATGGA-3'
MMP2_F	5'-GTGGGACAAGAACCAGATCAC-3'
MMP2_R	5'-GCATCATCCACGGTTTCAG-3'
MMP9_F	5'-ACGACATAGACGGCATCCA-3'
MMP9_R	5'-GCTGTGGTTCAGTTGTGGTG-3'
m_XRN1_F	5'-GGTCTTTATGCTTGGAACTCCTT-3'
m_XRN1_F	5'-AATCAAGTCTCCTGAATCCTGAA-3'
h_XRN1_F	5'-GCTGTACCACCTGGAACCAT-3'
h_XRN1_F	5'-CGACGAAGGCATTATATTAGCA-3'
m_DGCR8_F	5'-GGGGTTCCTTACTACGCATGT-3'
m_DGCR8_R	5'-CACACTCTTGTCAGAGGTCTCCT-3'
h_DGCR8_F	5'-TGCAAAGATGAATCCGTTGA-3'
h_DGCR8_R	5'-AGTAACTTGCTCAAAGTCAAAACG-3'

Supplementary References:

61. Garcia DM, Baek D, Shin C, Bell GW, Grimson A, Bartel DP. Weak seed-pairing stability and high target-site abundance decrease the proficiency of lsy-6 and other microRNAs. *Nat Struct Mol Biol* **18**, 1139-1146 (2011).

62. Kanehisa M, Goto S. KEGG: kyoto encyclopedia of genes and genomes. *Nucleic Acids Res* **28**, 27-30 (2000).

63. Dennis G, Jr.*, et al.* DAVID: Database for Annotation, Visualization, and Integrated Discovery. *Genome Biol* **4**, P3 (2003).

64. Fernandez JM, Hoffmann R, Valencia A. iHOP web services. *Nucleic Acids Res* **35**, W21-26 (2007).

65. Wingender E. The TRANSFAC project as an example of framework technology that supports the analysis of genomic regulation. *Brief Bioinform* **9**, 326-332 (2008).